Penerbit UTHM

© Universiti Tun Hussein Onn Malaysia Publisher's Office

JSMPM

http://publisher.uthm.edu.my/ojs/index.php/jsmpm

e-ISSN : 2821-2843

Journal of Sustainable Materials Processing and Management

Polymer Blends and Nanocomposite Materials Based on Polymethyl Methacrylate (PMMA) for Bone Regeneration and Repair

Zahra Al-Timimi[1*], Zeina J. Tammemi[2]

[1]Laser Physics Department, College of Science for Women,
University of Babylon, Hillah, 51001, IRAQ

[2]College of Dentistry,
University of Babylon, Hillah, 51001, IRAQ

*Corresponding Author

DOI: https://doi.org/10.30880/jsmpm.2022.02.01.002
Received 06 January 2022; Accepted 28 February 2022; Available online 26 April 2022

Abstract: As the population ages, so does the demand for bone loss treatments. The main components of these medicines must be able to endure longer and perform more effectively. Bone cement made of poly (methyl methacrylate) (PMMA), which is often used in damaged bone replacement surgery, is a vital biological material. As a result, the impact of additional nanoparticles such as zirconium dioxide ($Zr0_2$) and magnesium oxide (MgO) on polymer binary blends (Acrylic bone cement: 15% PMMA) for a bone scaffold was studied in this research. ZrO_2 and MgO nanoparticles were introduced in various weights present to the polymer mix matrix 0, 0.5, 1, 1.5, 2). Hand lay-up molding using two different types of PMMA material was utilized to create the polymer. The reinforcement materials were mixed individually with a binary polymer blend material according to the reinforcement material selection ratio, and then heat-treated at 55°C for 3 hours to complete polymerization and remove any residual stress. Mechanical characteristics such as tensile strength and Young's modulus were evaluated for all of the prepared samples. The chemical bonding of nanoparticles and synthetic binary polymeric mix composites was evaluated using Fourier transform infrared spectroscopy (FTIR). The tensile strength and Young's modulus of a binary polymeric blend reinforced with (1.5wt% ZrO_2, and 1wt% MgO) both dramatically increased. A scanning electron microscope (SEM) was used to examine the surface morphology of the fracture surface of tensile specimens. SEM images demonstrated that nanoparticles (ZrO_2 and MgO) were distributed uniformly throughout the polymeric mix matrix.

Keywords: ZrO_2, FTIR, polymer, MgO, polymeric blend matrix

1. Introduction

PMMA (poly (methyl methacrylate)) is a non-adhesive acrylic polymer used as bone cement in orthopedic implants. Chanley pioneered the orthopedic use of PMMA cement, which was the first cement to be used in spine applications, in the early 1960s [1,2]. For over 40 years, PMMA has been extensively studied as bone cement and is widely suitable for many injectable PMMA cement formulations engineered intended for vertebral body treatments because of its desirable features, such as appropriate strength to provide mechanical stability, moldable to fill complicated flaws, low cost, and FDA approval [3,4].

A polymer mixture is a type of material created by combining two or more polymers to create a new material with specific physical properties. They blend the alloy subsystems' features in a favorable way. The qualities of polymer blends are sometimes superior to those of their constituents. Polymer blending is a method of providing materials with

*Corresponding author: dr.altimimizahra@gmail.com

a comprehensive set of desired unique features at a cheap cost, such as a mix of toughness and strength, as well as solvent resistance [5,6].

Blending polymers is one of the most prevalent approaches for generating novel polymeric materials. Biopolymer composites are extremely important in tissue engineering for medical purposes because they provide a suitable environment for cell development and differentiation. Nano Zirconia (ZrO_2 nanoparticles) has recently gained a lot of attention due to its outstanding biocompatibility. The classification of ZrO_2 nanoparticles as a filler was based on their ability to improve the mechanical properties of acrylic resin [6,7]. ZrO_2 possesses several desirable properties, including high toughness and mechanical strength, abrasion and corrosion resistance, and biocompatibility. Nano ZrO_2 has excellent mechanical properties that make it resistant to crack propagation, and it is recognized to have the highest oxide hardness [8,9]. Magnesium oxide (MgO) is another bioactive substance that can be used as a PMMA additive because osteoblast adhesion to magnesium oxide-containing cement was significantly higher than adhesion to PMMA alone without affecting mechanical strength [10,11].

According to the review by Karageorgiou and Kapalan [12], changed forms of bone have distinct mechanical characteristics. Dependent on the direction in addition to the kind of the load, the mid-thigh cortical has a strength of 33-193 MPa and an elasticity modulus of 3-17 GPa. While the strength and elasticity modulus of the proximal femoral trabecular is 6.8 MPa and 0.441 GPa, respectively.

PMMA reinforced with 0, 0.5, 1, and 1.5 vol. % from MgO was created by Salih *et al.* [13]. The tensile strength and modulus of elasticity both improved dramatically. The mechanical characteristics of the PMMA matrix improved as the volume fraction of MgO in the matrix rose. Gad et al [14] used PMMA as a foundation material and added salinized ZrO_2 nanoparticles (40nm) to it 2.5, 5, and 7.5 wt %. The researchers looked at tensile strength and SEM tests. The results showed that as the wt % of ZrO_2 increased, the tensile strength increased as well. With the various ZrO_2 concentrations, the SEM micrographs revealed good surface properties.

The primary purpose of this study was to improve the mechanical properties of polymeric blends including ZrO_2 and MgO nanoparticles in accordance with bone tissue engineering standards. The biocompatible scaffold that closely resembles the extracellular matrix niche in genuine bone.

2. Materials and Methods

2.1 Materials

Acrylic bone cement for bone scaffold, which is a resin polymer produced by the Acro med Company, was used in this experiment. There are two parts to acrylic bone cement: a powder and a liquid. Methyl Methacrylate, Dimethyl-p-toluidine, and Ethylene glycol dimethyl acrylate (EGDMA) make up the liquid, while Ethylene glycol dimethyl acrylate (EGDMA) makes up the powder (PMMA). Self-curing Polymethylmethacrylate (PMMA), a type of acrylic resin, is manufactured by (ORT-365). It is separated into two parts: a translucent viscous liquid and a paste.

As reinforcement materials, two types of nanoparticles were utilized. The zirconium oxide (ZrO_2) powder, which was obtained with purity 99.9 % from Hongwu International Group Ltd, has a white color and an average diameter of 50.65 nm, while the yttrium oxide Y_2O_3 stabilized zirconia and magnesium oxide powder, which was obtained with purity 99.9 % from Beijing DK nanotechnology has a white color and an average diameter of 68.83 nm.

2.2 Polymer Mixes and Composite Samples Preparation

Hand lay-up molding using two different types of PMMA material was utilized to create the polymer. Acrylic bone cement specimens were made by combining 3.5 wt % from the liquid component of the Methyl methacrylate (MMA) monomer with 5 wt % from powders to make acrylic bone cement specimens. According to the manufacturer's specifications for the PMMA material, the acrylic resin and hardener should be mixed at a ratio of 100:2. As a result, the control group was made with a weighed amount of acrylic bone cement as a base ingredient, blended with PMMA at a 15 wt %, and manually mixed until the mixture was homogeneous. The mixture was poured into the mold to obtain the final standardized samples. The mixture was then allowed to harden for 48 hours at room temperature in the mold. After that, the casting sample is heated for 3 hours at 50 °C. Finally, it was left at ambient temperature for 72 hours to complete polymerization.

2.3 Composites Preparation

The weights of the reinforcement components are determined by the weight fractions of the strengthening materials ($Zr0_2$ and MgO) in the proper selection ratio. Essentially, the nanoparticle powders were estimated using an electronic balance, based on the overall weight of the matrix material (polymer binary mixes) (Acrylic bone cement: 15 % PMMA). The reinforcement materials were mixed individually with a binary polymer blend material according to the reinforcement material selection ratio, and then heat-treated at 55 °C for 3 hours to complete polymerization and remove any residual stress caused by the de-molding of the samples into the metal mold cavity.

2.4 FTIR Spectroscopy

The test was performed using a Bruker/Tensor 27 FTIR in accordance with the [E1252-98(2021)]-Standard practice designed for general techniques used for obtaining infrared spectra in support of qualitative analysis [15]. It has a Digi Tech TM detector system, DLATGS with high sensitivity, and a spectral range of 4000-400 cm^{-1} with a standard KBr beam splitter.

2.5 Mechanical Properties

The tensile tests were conducted in accordance with ASTM D638 standards [16,17]. The sample length was 165 mm, and the thickness was 7 mm. A Universal tensile test machine with a load capacity of 50 kN in addition to a crosshead velocity of 5 mm/min had been used to conduct the tensile test. The Young's modulus and ultimate strength of materials with varying filler weight percentages were computed for modulus of elasticity evaluation and comparison.

3. Results and Discussion

The Fourier transform infrared spectroscopy (FTIR) of acrylic bone cement and type PMMA are shown in Fig. 1(a) and Fig. 1(b), respectively. The wide peak (4000-2900 cm^{-1}) corresponds to the appearance of stretching vibration, while the peak 2961.29 cm^{-1} corresponds to the C-H stretch of the methyl group (CH_3). PMMA's main distinctive vibration bands are sharp intense peaks as a result of C=O stretching is caused by the presence of an ester carbonyl group (1745.87 cm^{-1}) [15,18].

The 1457.16 cm^{-1} and 1280.78 cm^{-1} bands relate to C-H symmetric and asymmetric stretching modes, respectively, and the large peak extending from 1488-1000 cm^{-1} can be explained by the stretching vibration of the C-O (ester bond). The peak at 1280.78 cm^{-1} corresponds to methylene group CH_2 torsion, the peak at 1195 cm^{-1} to -O-CH_3 stretching vibrations, and the peak at 864.21 cm^{-1} to the C-C stretching band [19,20].

Fig. 1(c) shows the infrared spectrum of the binary polymer mix (acrylic bone cement: 15 % PMMA) as ideal samples. All the characteristic vibration bands of the acrylic bone cement illustrated in Fig. 1(a) is present in FTIR spectra of binary polymer blends. These spectra also revealed that the peak at 2920.07 cm^{-1} corresponds to the C-H stretching band of the methyl group (CH_3).

The primary distinctive vibration bands of acrylic bone cement include the stretching vibration C=O band (1722.57 cm^{-1}), the stretching vibration ester bond C-O band (1434.69 cm^{-1}), and the symmetric and asymmetric stretching modes of the C-H band (1386.51 cm^{-1}). The methylene group torsion band CH_2 has a peak of 1239.41 cm^{-1}, while the stretching band C-C has a peak of 986.85 and 840.58 cm^{-1} [21].

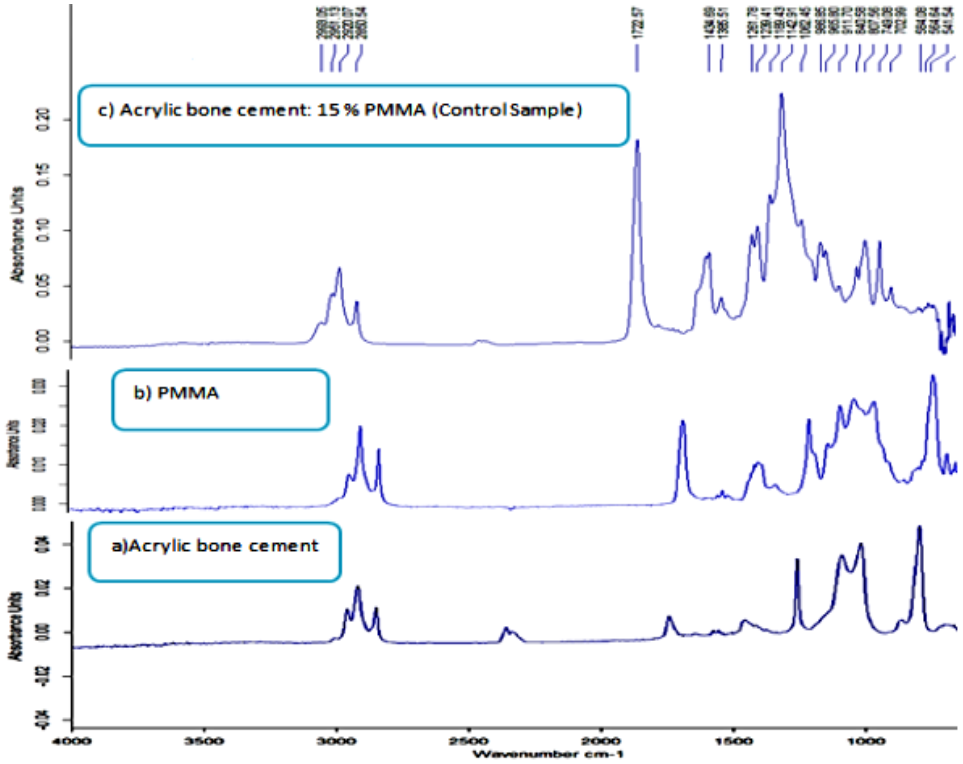

Fig. 1 - FTIR spectra: a) acrylic bone cement, b) PMMA, and c) polymer blends (acrylic bone cement: 15 % PMMA)

Fig. 2 shows the infrared spectra of a binary polymer blend (acrylic bone cement: 15 % PMMA) (control sample) and polymer blend composites augmented with various ratios of ZrO_2 nanoparticles. PMMA principal vibration band characteristics occur at the C=O band (1723.97 cm^{-1}), and fingerprint peaks at the C-O band (1434.69 cm^{-1}). Because of the presence of ZrO_2 particles in PMMA, the bands assigned to the Zr-O, and O-Zr-O bands in ZrO_2 weakened and eventually vanished [22,23]. There were no new peaks or peak shifts in the infrared spectra of (acrylic bone cement: 15 % PMMA) composites specimens. This is owing to the lack of cross-linking in these specimens and the need to find a physical bond. At 0.5 wt %. percent ZrO_2, all typical peaks show a noticeable decrease in peak intensity, which then increases with increasing ZrO_2 content in PMMA composites specimens.

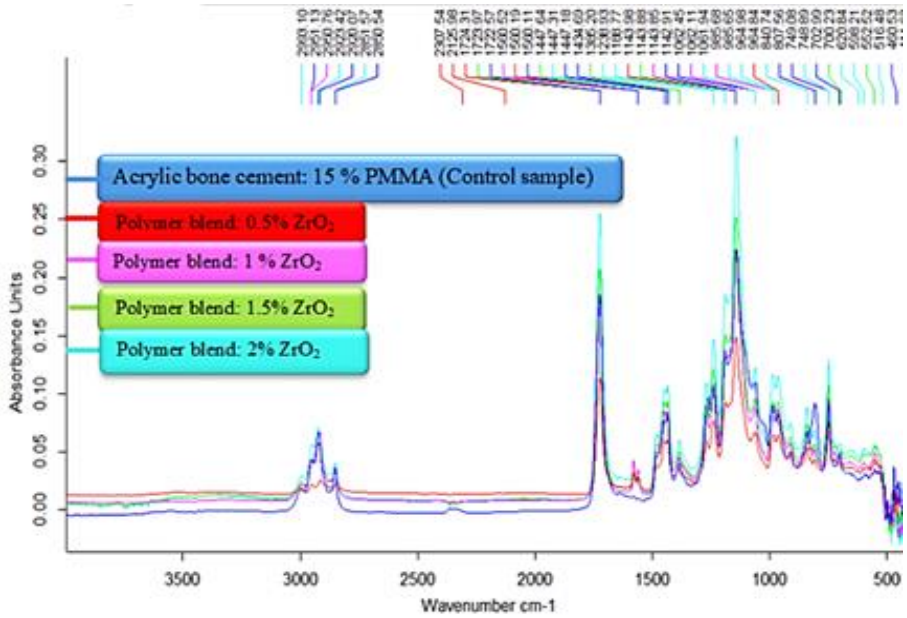

Fig. 2 - FTIR spectra of the first group bio-composites (acrylic bone cement: 15 % PMMA), with the composite content of ZrO_2 nanoparticles as a variable

Fig. 3 shows the FTIR spectrum of a binary polymer blend (acrylic bone cement: 15 % PMMA) and its polymer blend composites augmented with various MgO nanoparticle content ratios in the composite. The C=O band (1722.57 cm^{-1}) and the fingerprint peak (1434.69 cm^{-1}) for C-O band vibration are the major characteristics of the acrylic bone cement vibration band. The presence of MgO nanoparticles in a polymer mixture weakened the bands attributed to Mg-O and Mg-O-Mg compounds in the 661.01–511.18 cm^{-1} range as a wideband [24,25].

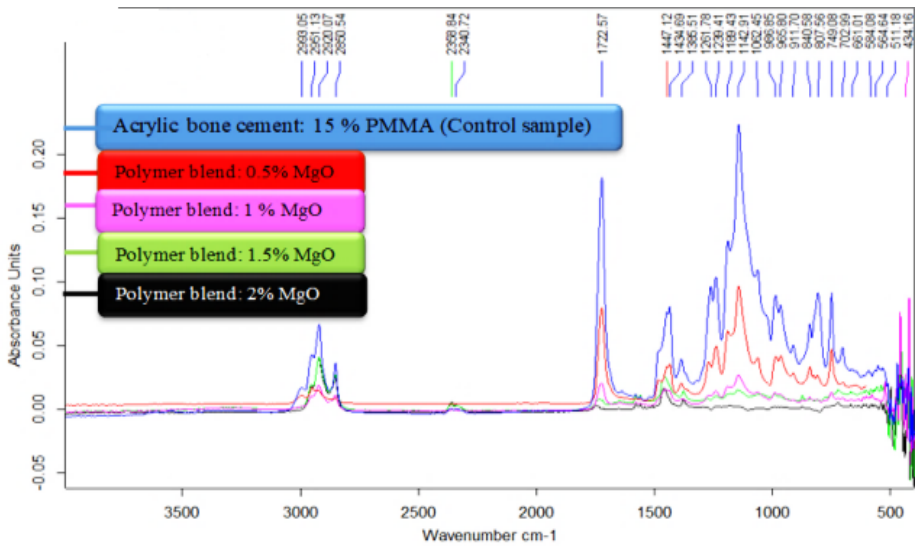

Fig. 3 - FTIR spectra of the second group bio composites (Acrylic bone cement: 15 % PMMA), with the composite content of MgO nanoparticles as a variable

Fig. 4 and Fig. 5 depict the stress-strain behavior of composite materials made up of a polymeric blend (acrylic bone cement: 15 % PMMA) reinforced with three different types of nanoparticles of ZrO_2 and MgO at different weight % fractions (0.5, 1, 1.5, 2).

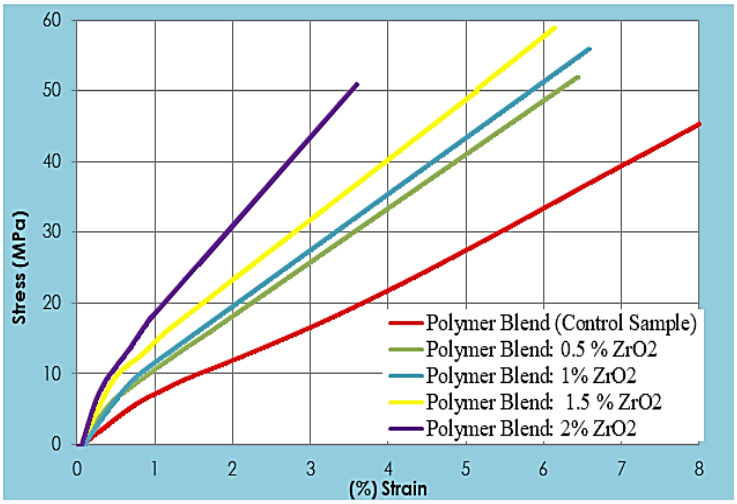

Fig. 4 - Stress-strain curve for the bio composite (acrylic bone cement: 15 % PMMA), a function of the ZrO_2 content in the composite

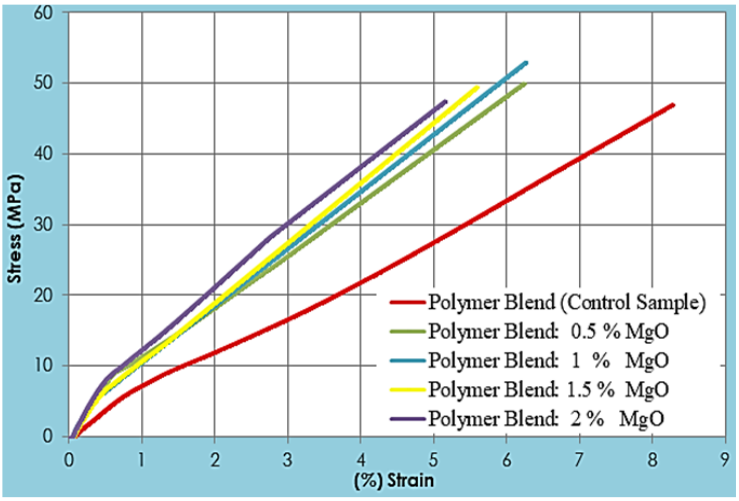

Fig. 5 - Stress-strain curve for the bio composite (acrylic bone cement: 15 % PMMA), a function of the MgO content in the composite

The modulus of elasticity and fracture strength for three sets of hybrids are shown in Fig. 6 and Fig. 7, respectively. As a result of the nanoparticle (ZrO_2 and MgO) contents in the mixture, nanocomposite samples (acrylic bone cement: 15 % PMMA nanoparticles) were created. In comparison to the polymeric mix, increasing the weight fraction up to 1.5 wt % of ZrO_2 increased the tensile strength by 26 % and 12 % for 1 wt % of MgO, respectively.

This increase in strength can be explained by the strengthening caused by the presence of uniformly distributed tougher and stronger particles in the matrix. Furthermore, nanoparticles' vast surface area provides more points of interaction with polymer blends and nano additives, improving mechanical interlocking and allowing a shift in the polymer mixture's properties. Furthermore, the nanoparticles have already established a well-distributed transfer of stress from the matrix to the strong nanofillers. Finally, the polymeric blend reinforced with 1.5 wt % ZrO_2 exhibits good mechanical properties and the addition of ZrO_2 nanoparticles to the polymeric blend adds to the improvement of mechanical properties. This may be due to ZrO_2 intrinsic strength when compared to other nanoparticles.

However, the polymeric blend composites samples with 1.5 wt %. percent ZrO_2 and 1 wt % MgO nanoparticle had greater young's modulus values, as shown in Fig. 7. Furthermore, the polymeric blends reinforced by ZrO_2 nanoparticles have a higher elastic modulus than their counterparts in the other groups' composite samples, as shown in

this figure. This behavior can be explained by ZrO_2 inherent property of high mechanical strength, which increases the mechanical properties of acrylic mix-based composites [22,26].

When the number of nanoparticles (ZrO_2, and MgO) is increased, the interfacial adhesion between the components appears to decrease, and a non-homogeneous distribution results in composites with reduced elastic modulus.

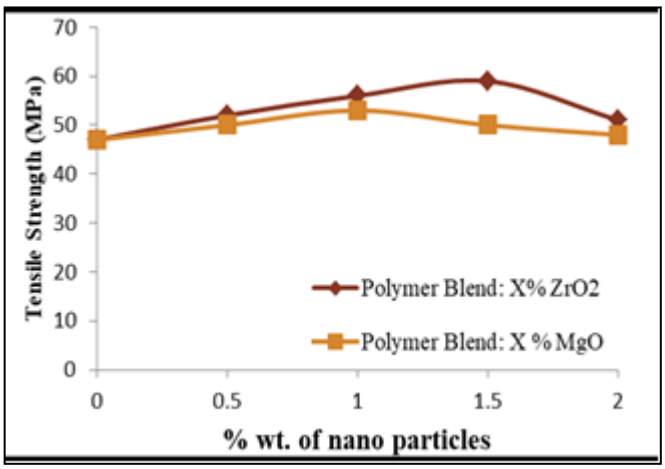

Fig. 6 - Tensile strength of a bio composite (acrylic bone cement: 15 % PMMA) as a function of the quantity of nanofillers (ZrO_2 and MgO) in the mixture

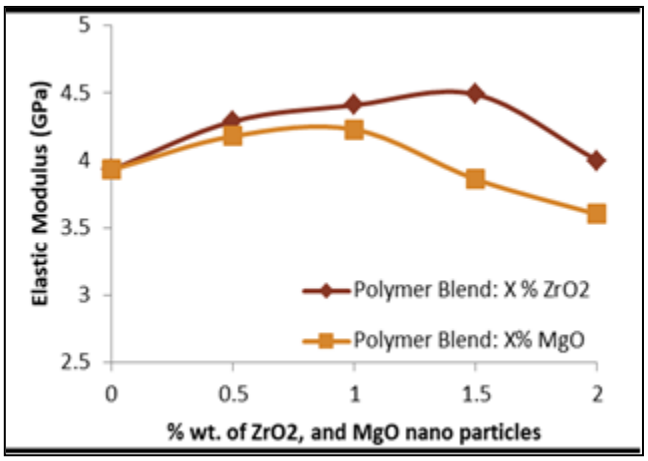

Fig. 7 - Modulus of elasticity of a bio composite (acrylic bone cement: 15 % PMMA) as a function of the quantity of nanofillers (ZrO_2 and MgO) in the mixture

The addition of the fillers 2 wt % ZrO_2 and < 1. 5 wt % MgO to the nanohybrid composites resulted in a drop in tensile strength. The dispersion process is rendered ineffective due to the presence of particle-matrix interfacial defects and the presence of Vander Waals forces. Furthermore, the presence of agglomerated fillers that form loosely connected clusters that influence the fracture propagation mode reduces the tensile strength of the material [27,28].

The mechanical and physical properties of a composite are directly influenced by the size, quantity, and dispersion of the reinforcing phase, as well as interfacial bonding between the components. They also have an impact on the morphology of composite microstructures. To connect the mechanical properties of polymers blending samples with their microstructural morphologies, micrograph investigations using scanning electron microscopy (SEM) were performed on the fracture surfaces at magnification 1000X.

The fracture surface morphology was studied for binary polymer mixing (control sample), polymer nanocomposite of ((acrylic bone cement: 15 % PMMA): 1.5 % ZrO_2), and ((acrylic bone cement: 15 % PMMA): 1 % MgO). All microstructural morphologies appeared as co-continuous structures, making it more difficult to discriminate between separate polymers in these polymeric blends' composites. Fig. 8 indicates that composite specimen components with added nano-sized reinforcing materials 1.5 % ZrO_2 and 1 % MgO to binary polymeric mix had greater interfacial adhesion. The fracture surface of polymeric composites, on the other hand, was rough and uneven, with a pattern of ductile dimples. Furthermore, the architecture of the fracture surface revealed lamellar steps of very uniform size and distribution, which are typical of ductile fractures [29,30].

Furthermore, there was no large aggregation of these nanoparticles that showed a consistent particle dispersion. Most nanoparticles' fracture surface morphology is integrated as an inherent component of the matrix material of the base material structure, which is a favorable sign compatibility between the matrix material and leading to the formation of strong physical bonding (strong interfacial regions) between the nanoparticles and polymeric blending matrix [31,32]. Most nanoparticles' fracture surface morphology is as an intrinsic component embedded inside the matrix material of the base material structure, showing that it is in good condition compatibility between the matrix material and leading to the formation of strong physical bonding (strong interfacial regions) between the nanoparticles and polymeric blending matrix [33,34].

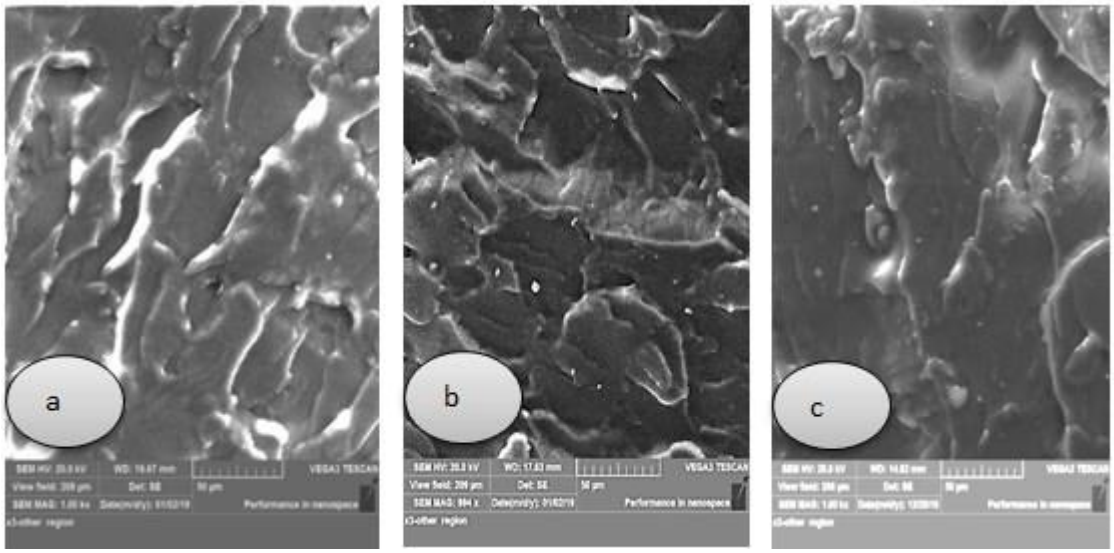

Fig. 8 - SEM images: (a) binary polymer blend (acrylic bone cement: 15 % PMMA (control sample)), (b) (acrylic bone cement: 15 % PMMA): 1.5 % ZrO_2), and (c) (acrylic bone cement: 15 % PMMA): 1 % MgO)

4. Conclusion

When compared to other reinforcing nanoparticle materials (MgO) utilized in this work, adding ZrO_2 nanoparticles to a polymer mixture (acrylic bone cement: 15 % PMMA) resulted in higher mechanical properties (tensile strength in addition to Young's modulus). Young's modulus and tensile strength of polymeric blend nanocomposites samples were also improved when nanoparticles were introduced to a particular limit (1.5 wt % ZrO_2) and (1 wt % MgO). Finally, when the nanoparticles were added above a certain limit in the composite, the mechanical characteristics were reduced, but they were kept better than in the polymer blend as a foundation material. As a result, these samples could be made from materials that have the characteristics needed for bone scaffold applications.

Acknowledgement

The authors are grateful to the University of Babylon for providing academic, moral, and laser laboratory support. Thank you to the entire technical staff at the Women's Science Colleges Laser Department.

References

[1] Kausar, A. (2019). Corrosion prevention prospects of polymeric nanocomposites: A review. *Journal of Plastic Film & Sheeting*, *35*(2), 181-202.

[2] Hentschel, L., Kynast, F., Petersmann, S., Holzer, C., & Gonzalez-Gutierrez, J. (2020). Processing conditions of a medical grade poly (methyl methacrylate) with the arburg plastic freeforming additive manufacturing process. *Polymers*, *12*(11), 2677.

[3] Alsulami, Q. A., & Rajeh, A. (2022). Structural, thermal, optical characterizations of polyaniline/polymethyl methacrylate composite doped by titanium dioxide nanoparticles as an application in optoelectronic devices. *Optical Materials*, *123*, 111820.

[4] Dhatarwal, P., Sengwa, R. J., & Choudhary, S. (2022). Broadband Radio Frequency Dielectric Permittivity and Electrical Conductivity of Dispersed Tin Oxide and Silica Nanoparticles in Poly (Ethylene Oxide)/Poly (Methyl Methacrylate) Blend Matrix-Based Nanocomposites for Nanodielectric Applications. *Journal of Macromolecular Science, Part B*, *61*(2), 111-120.

[5] Zhong, M., Chai, L., Wang, Y., & Di, J. (2021). Enhanced efficiency and stability of perovskite solar cell by adding polymer mixture in perovskite photoactive layer. *Journal of Alloys and Compounds*, *864*, 158793.
[6] Poon, W. C. K. (2002). The physics of a model colloid–polymer mixture. *Journal of Physics: Condensed Matter*, *14*(33), R859.
[7] Ahangaran, F., Navarchian, A. H., & Picchioni, F. (2019). Material encapsulation in poly (methyl methacrylate) shell: A review. *Journal of Applied Polymer Science*, *136*(41), 48039.
[8] Ahmed, M. A., & Ebrahim, M. I. (2014). Effect of zirconium oxide nano-fillers addition on the flexural strength, fracture toughness, and hardness of heat-polymerized acrylic resin. *World journal of nano science and engineering*, 4, 50–57.
[9] Gad, M. M., Abualsaud, R., Rahoma, A., Al-Thobity, A. M., Al-Abidi, K. S., & Akhtar, S. (2018). Effect of zirconium oxide nanoparticles addition on the optical and tensile properties of polymethyl methacrylate denture base material. *International Journal of Nanomedicine*, *13*, 283-292.
[10] Hickey, D. J., Ercan, B., Sun, L., & Webster, T. J. (2015). Adding MgO nanoparticles to hydroxyapatite–PLLA nanocomposites for improved bone tissue engineering applications. *Acta Biomaterialia*, *14*, 175-184.
[11] Hegazy, E. S. A., Ghaffar, A. M. A., & Ali, H. E. (2020). Characterization and radiation modification of low density polyethylene/polystyrene/maleic anhydride/magnesium hydroxide blend nanocomposite. *Materials Chemistry and Physics*, *252*, 123204.
[12] Karageorgiou, V., & Kaplan, D. (2005). Porosity of 3D biomaterial scaffolds and osteogenesis. *Biomaterials*, *26*(27), 5474-5491.
[13] Salih, S. I., Oleiwi, J. K., & Abd Alkhidhir, S. (2018). Comparative Study of Some Mechanical Properties of Hybrid Polymeric Composites Prepared by using Friction Stir Processing. *Journal of Advanced Research in Dynamic and Control Systems*, *10*(2), 1316-1326.
[14] Pansieri, J., Plissonneau, M., Stransky-Heilkron, N., Dumoulin, M., Heinrich-Balard, L., Rivory, P., ... & Marquette, C. (2017). Multimodal imaging Gd-nanoparticles functionalized with Pittsburgh compound B or a nanobody for amyloid plaques targeting. *Nanomedicine*, *12*(14), 1675-1687.
[15] Nan, C., Yue, W., Wang, B. Y., Yang, X., & Tao, L. (2021). Research on numerical model of nano-FTIR system based on COMSOL. *Spectroscopy and Spectral Analysis*, *41*(4), 1125-1130.
[16] Ankersen, J., Birkbeck, A. E., Thomson, R. D., & Vanezis, P. (1999). Puncture resistance and tensile strength of skin simulants. *Proceedings of the Institution of Mechanical Engineers, Part H: Journal of Engineering in Medicine*, *213*(6), 493-501.
[17] Luo, S., He, W., Chen, K., Nie, X., Zhou, L., & Li, Y. (2018). Regain the fatigue strength of laser additive manufactured Ti alloy via laser shock peening. *Journal of Alloys and Compounds*, *750*, 626-635.
[18] Khan, A., Khan, G. H., Mirza, E. H., Chandio, A., Mohsin, M., Hassan, M., ... & Jafri, A. R. (2022). Development and Characterization of Acrylic Based Bone Cements. *Journal of Biomaterials and Tissue Engineering*, *12*(3), 471-479.
[19] Wang, H., Maeda, T., & Miyazaki, T. (2021). Preparation of bioactive and antibacterial PMMA-based bone cement by modification with quaternary ammonium and alkoxysilane. *Journal of Biomaterials Applications*, *36*(2), 311-320.
[20] Dubey, U., Kesarwani, S., Kyratsis, P., & Verma, R. K. (2022). Development of modified polymethyl methacrylate and hydroxyapatite (PMMA/HA) biomaterial composite for orthopaedic products. *Advances in Product Design Engineering*, 159-178.
[21] Sahu, D. K., Rai, J., Rai, M. K., Banjare, M. K., Nirmal, M., Wani, K., ... & Mundeja, P. (2020). Detection of flonicamid insecticide in vegetable samples by UV–Visible spectrophotometer and FTIR. *Results in Chemistry*, *2*, 100059.
[22] Baciu, D. E., & Simitzis, J. (2013). Synthesis and characterization of acrylic bone cement reinforced with calcium carbonate-bioceramic. *Journal of Optoelectronics and Advanced Materials*, *15*(March-April 2013), 145-149.
[23] Salih, S. I., Salih, W. B., & Mohammed, M. S. (2018). Preparation and investigation of flexural strength and impact strength for nano hybrid composite materials of the tri-polymeric blend used in structural applications. *Engineering and Technology Journal*, *36*(1 Part B), 12-24.
[24] Sadeq, H. M., Salih, S. I., & Braihi, A. J. (2019). Development of surface roughness and mechanical properties of PMMA nanocomposites by blending with polymeric materials. *Engineering and Technology Journal*, *37*(12), 558-565.
[25] Cossu, C. M. F. A., Pais Alves, M. F. R., de Assis, L. C. L., Magnago, R. D. O., de Souza, J. V. C., & dos Santos, C. (2018). Development and characterization of Al2O3-ZrO2 composites using ZrO2 (Y2O3)-recycled as raw material. *Materials Science Forum*, 912, 124-129.
[26] Remzova, M., Zouzelka, R., Brzicova, T., Vrbova, K., Pinkas, D., Rőssner, P., ... & Rathousky, J. (2019). Toxicity of TiO2, ZnO, and SiO2 nanoparticles in human lung cells: Safe-by-design development of construction materials. *Nanomaterials*, *9*(7), 968.
[27] Kain, V. (2012). Corrosion-resistant materials. *Funct. Mater.* 507–547.

[28] Ramachandran, M., Bhargava, R., & Raichurkar, P. P. (2016). Effect of nanotechnology in enhancing mechanical properties of composite materials. *International journal on Textile Engineering and Processes*, *2*(1), 59-63.
[29] Ye, C., Suslov, S., Lin, D., Liao, Y., Fei, X., & Cheng, G. J. (2011). Microstructure and mechanical properties of copper subjected to cryogenic laser shock peening. *Journal of Applied Physics*, *110*(8), 083504.
[30] Kim, M. J., & Sun, X. S. (2015). Correlation between physical properties and shear adhesion strength of enzymatically modified soy protein-based adhesives. *Journal of the American Oil Chemists' Society*, *92*(11), 1689-1700.
[31] Abdullah, H. Z., Lee, T. C., Idris, M. I., & Selimin, M. A. (2020). Bio-ceramics for tissue engineering. In *Tissue Engineering Strategies for Organ Regeneration*, pp. 126-143. CRC Press.
[32] Bailey, E. J., & Winey, K. I. (2020). Dynamics of polymer segments, polymer chains, and nanoparticles in polymer nanocomposite melts: A review. *Progress in Polymer Science*, *105*, 101242.
[33] Wu, H., Fahy, W. P., Kim, S., Kim, H., Zhao, N., Pilato, L., ... & Koo, J. H. (2020). Recent developments in polymers/polymer nanocomposites for additive manufacturing. *Progress in Materials Science*, *111*, 100638.
[34] Zhang, M., Song, W., Tang, Y., Xu, X., Huang, Y., & Yu, D. (2022). Polymer-based nanofiber–nanoparticle hybrids and their medical applications. *Polymers*, *14*(2), 351.